MASS TRANSPORT AND ATHEROSCLEROSIS IN MOVING CORONARY ARTERIES. A CFD STUDY

M.K. Kolandavel*, E.T. Fruend**, S. Ringgaard** and P.G. Walker*

* School of Mechanical Engineering, University of Leeds, Leeds LS2 9JT, UK
** Institute of Clinical Medicine and MR-Research Centre, Skejby Hospital, Skejby Sygehus, Aarhus N, Denmark 8200

men1kkm@leeds.ac.uk

Abstract: In this study we hypothesise that the mass transport of low density lipoprotein (LDL) and oxygen in coronary arteries may be affected by their physiological motion, a factor which has not been considered widely in mass transfer studies. Hence, species transport in an idealized moving coronary artery model was investigated computationally. Due to the differences in LDL and oxygen transport the respective transport processes were modelled as concentration polarisation and first order wall reaction. Simulations were carried out under steady and pulsatile flow conditions in static and dynamic models with a physiological inlet velocity and a sinusoidal wall motion waveform. The results predicted co-localisation of low wall shear stress (WSS), high LDL flux and low oxygen flux along the inner wall of curvature, a predilection site for atherosclerosis. The temporal variations in flow and the WSS patterns due to the flow pulsation and wall motion did not produce time dependent changes in the oxygen and LDL wall flux. Nevertheless, the wall motion altered time-averaged oxygen and LDL flux in the medial and distal regions. Taken together, these results seem to suggest that the wall motion may play an important role in coronary arterial transport processes and the formation of atherosclerotic plaques.

Introduction

The transport of blood-borne species to the arterial wall and their accumulation within the arterial wall has been related to the formation of atherosclerosis [1], the number one killer disease in the West. Of all the transport processes, the transport of LDL is of paramount importance because LDL accumulation within the arterial wall is a hallmark of early atherosclerosis [2]. Of equal importance is the oxygen transport as it is not only essential for the normal arterial wall metabolism but low oxygen tension (hypoxia) in the arterial wall can increase the wall permeability of macromolecules including LDL [1].

The local susceptibility of coronary arteries to atherosclerosis has been putatively linked to the physiological motion arising out of their anatomical attachment to the epicardial surface of the beating heart [3]. This raises a possibility that in coronary arteries oxygen and LDL transport may be affected by the wall motion, a factor which has not been considered widely in mass transfer studies. Therefore, this study was initiated to investigate the transport of LDL and oxygen in a dynamically curved 3-D model of the left anterior descending coronary artery (LAD) segment by using the commercial finite volume CFD solver, FLUENT (v6.1.22, Fluent Inc, Lebanon, NH).

Methods

A 3-D finite volume model of a simplified LAD was created using the CFD pre-processor GAMBIT (v2.1.6, Fluent Inc). The characteristic LAD geometry and flow conditions applied to the simulations were: mean radius of curvature (R) = 4cm, diameter (d) =0.36cm, length (l) =4.68cm, mean velocity (v) =9.715cm/s, mean Re =105, mean Dean number (κ) =22.3 and a Womersley number of 2.78 corresponding to a cardiac cycle duration (T) of 0.8s [4-6]. The model was assumed to be rigid with a circular cross section of constant radius and a constant uniplanar curvature over its entire length at any instant.

A published pulsatile inlet velocity waveform [7] was imposed at the inlet boundary (Fig. 1). A fully developed flow assumption was used at the inlet. Blood was assumed to be an incompressible, Newtonian fluid with a density and viscosity of 1050kg/m^3 and 0.0035Pa.s. The radius of curvature of the model was varied sinusoidally (Fig. 1) at a frequency of 1.25Hz based on a model developed by Santamarina et al [8].

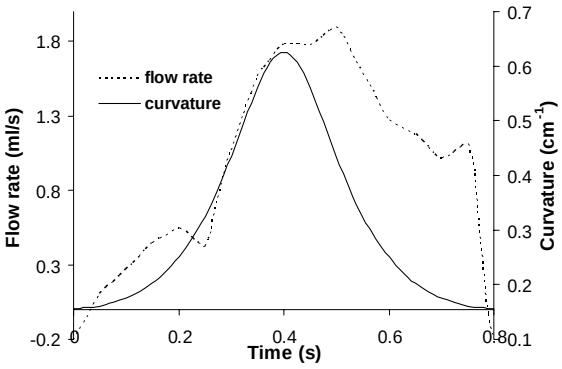

Figure 1: The LAD inlet flow and curvature waveforms.

$$R(t) = R_{mean}\left[1 + \varepsilon.\cos(\omega t)\right] \quad (1)$$

ISSN: 1727-1983

where ω is the angular frequency of deformation and ε is the physiological deformation parameter of 0.6 [8] corresponding to R_{max} and R_{min} values of 6.4cm and 1.6cm respectively.

$$\varepsilon = \frac{(R_{\max} - R_{\min})}{R_{mean}} \quad (2)$$

The mass transport of species in the arterial lumen is mathematically described using the three dimensional convection-diffusion equation

$$\frac{\partial C}{\partial t} + \mathbf{u}.\nabla C - D\nabla^2 C = 0 \quad (3)$$

where C is the concentration of species, **u** is the velocity vector and D is the diffusivity of species in the blood.

The semi-permeable endothelial layer acts as a barrier for the entry of macromolecules such as LDL into the arterial wall. In contrast, it allows the blood plasma and small solutes such as oxygen to filter through its monolayer to gain entry into the arterial wall. Hence it is appropriate to use different wall boundary conditions to model LDL and oxygen transport to the wall. The other mass transfer boundary conditions were uniform inlet mass fraction (oxygen = 0.005 & LDL = 0.0011) [9, 10] and a zero gradient in concentration at the outlet.

LDL wall boundary condition used was simply mass conservation at the endothelial surface [11] described as

$$-D\frac{\partial C}{\partial \mathbf{n}} = (K - Vw)Cw \quad (4)$$

where Vw is the plasma filtration velocity normal to the wall (=4x10^{-6}cm/s) [12], Cw is the endothelial surface concentration of LDL, **n** is the unit vector normal to the vessel wall, D is the physiological LDL diffusivity (=5x10^{-8}cm^2/s) [13] and K is the overall mass transfer coefficient of LDL which was considered equivalent to physiological endothelial permeability of LDL (=2x10^{-8}cm/s) [14]. For oxygen transport a constant permeability wall boundary condition was applied

$$-D\frac{\partial C}{\partial \mathbf{n}} = KCw \quad (5)$$

where oxygen diffusivity and permeability were 1x10^{-5}cm^2/s [15] and 2x10^{-3}cm/s [16] respectively.

The commercial parallel CFD solver FLUENT (v6.1.22, Fluent Inc.) was used to model LDL transport in the moving LAD model. Fluent uses a finite volume technique to solve the three dimensional (3-D) unsteady equations of momentum, mass and species conservation. The wall motion was implemented through the arbitrary Lagrangian-Eulerian formulation. At each time step the volume mesh was updated through a user defined function. At the beginning of each simulation, the radius of curvature of the model was at its maximum. At t=0.2s and 0.6s the radius of curvature of the model was equivalent to R_{mean}. The inlet was fixed in the simulation so that the centre of curvature was allowed to vary sinusoidally according to Eq. 1.

The computational method was validated by simulating Santamarina et al's [8] coronary artery motion study in a curved model of exactly similar dimensions under identical flow and wall motion conditions. The mesh and time step independence of the solutions were investigated by successively refining the grid and the time step size by a factor of two until solution convergence. Based on these criteria a mesh containing 156,861 nodes with a time step size of 0.0125s was chosen as the optimum case for simulation. The results of our validation tests have been presented in detail in our previous article [17].

Results

The axial and secondary velocity vector plots in the static and dynamic models showed velocity skewing towards the outer wall due to vessel curvature and the appearance of Dean vortices in the cross sectional planes. Although both the pulsatility and wall motion produced time dependent velocity skewing the flow pulsation had a greater effect on velocity skewing than the wall motion. When both the wall motion and pulsatility were considered there was a reduction in velocity skewing over the entire cycle and a reduction in secondary flow when the vessel curvature was small and vice versa during the peak curvature phases. Nevertheless, the velocity skewing as well as secondary flow increased with increase in curvature and flow rate.

The pulsatility of blood flow caused time dependent WSS distribution. The WSS increased with flow rate and this increase was greater along the outer wall. Consequently, the WSS curve was seen to follow the flow rate curve (Fig. 1). When the wall motion was introduced the instantaneous variations in the outer and inner WSS were somewhat similar to that caused by the flow pulsation. However, the dynamic curvature effects were evident in the central section where the location and magnitude of peak WSS were different. Nevertheless, the outer WSS was higher than the inner WSS in both the models.

The time-averaged WSS distribution exhibited notable spatial variations (Fig. 3). In general, the time-averaged outer WSS was higher than the inner WSS at all axial locations. The flow pulsation caused an increase in the time-averaged outer WSS to its peak value and a gradual decrease afterwards. When the wall motion was included the peak WSS was higher and there was a steeper drop in the time-averaged outer WSS after peaking. Along the inner wall the dynamic WSS was generally higher than the static WSS and a region of minimum WSS was also noted.

The oxygen transport results concern the prediction of non dimensional oxygen flux (KCw/KCo) to the LAD wall (Fig. 4 & 5). The oxygen flux was only found

ISSN: 1727-1983

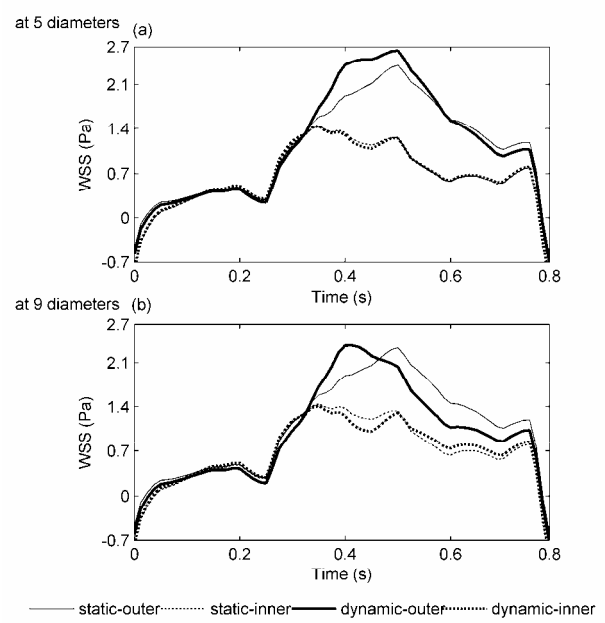

Figure 2: Temporal axial inner and outer WSS distribution at 5 and 9 diameters in the LAD.

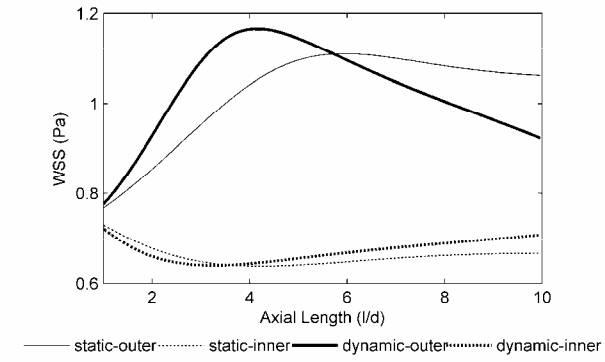

Fig. 3 Time-averaged axial WSS distribution along the inner and outer walls of the LAD.

to exhibit minor time dependent variations (Fig. 4). This was evident in the central section. In both the static and dynamic models, the inner wall oxygen flux was always lower than that to the outer wall. Over all there was an increase in oxygen flux due to wall motion along the inner wall. This increase was greater in the distal regions. However, the wall motion induced outer wall oxygen flux was higher in the proximal and medial regions and lower in the distal regions when compared to the flux distribution in the static model.

The time-averaged non dimensional oxygen wall flux distribution is shown in Fig. 5. The flow pulsation led to a drop in the inner wall oxygen flux from the inlet to the outlet. When the wall motion was introduced the inner wall oxygen flux was more than that caused by the flow pulsatility. Moreover, the difference in fluxes increased with distance from the inlet due to an increase in the time-averaged inner wall oxygen flux. Along the outer wall the pulsatility of flow caused a sharp drop in oxygen flux in the proximal region followed by a gradual increase and decrease in the medial and distal regions. When the wall motion was included the outer wall oxygen flux closer to the inlet was also found to drop sharply. However, the increase in flux was greater in the medial region and the subsequent decrease in flux was sharper than in the static model.

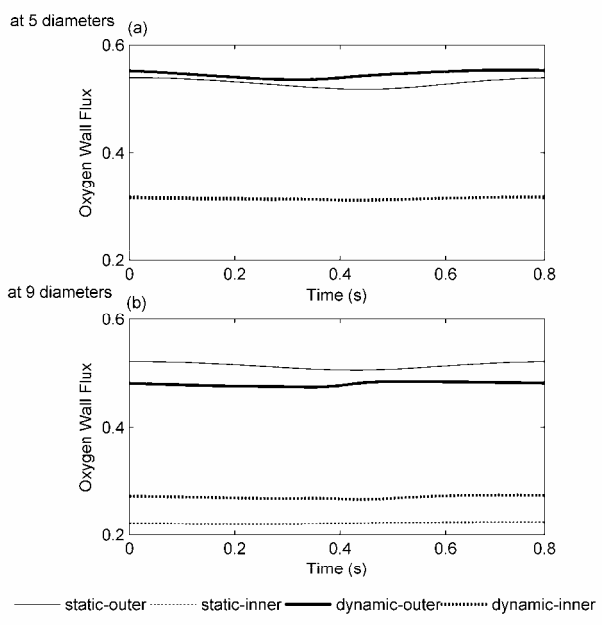

Figure 4: Temporal normalised oxygen flux to the inner and outer walls at 5 and 9 diameters in the LAD.

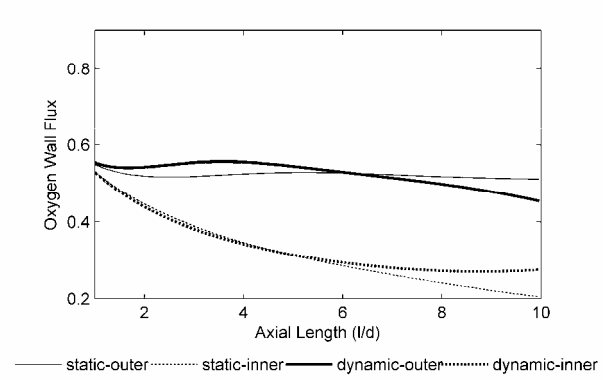

Figure 5: Time-averaged normalised oxygen wall flux distribution along the outer and inner walls.

The non dimensional LDL wall flux (KCw/KCo) at 5D and 9D is plotted in Fig. 6. Neither the wall motion nor the flow pulsatility produced temporal variations in LDL wall flux. The flow pulsation caused higher LDL flux to the inner wall and lower flux to the outer wall. The wall motion caused a reduction in LDL flux to the inner wall and this reduction was more prominent in the distal regions. Along the outer wall the effects of wall motion were to decrease the LDL flux in the proximal and medial regions and to increase the LDL flux in the distal region.

ISSN: 1727-1983

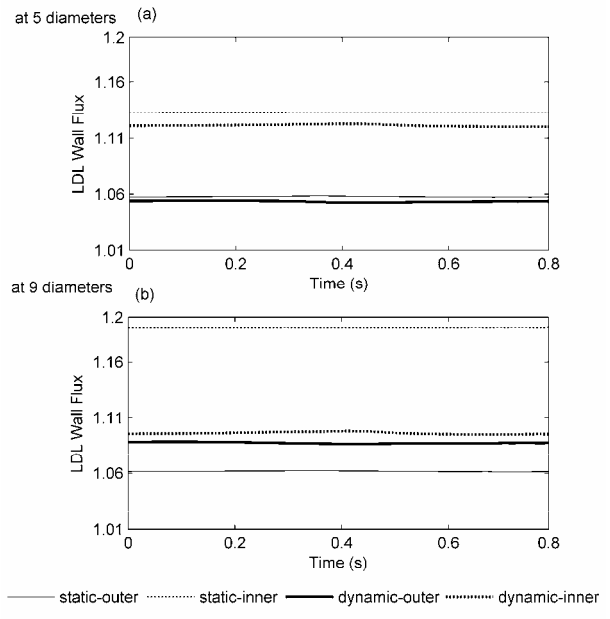

Figure 6: Temporal normalised LDL flux to the inner and outer walls at 5 and 9 diameters in the LAD model.

The time-averaged non dimensional LDL wall flux distribution is shown in Fig. 7. Both the wall motion and flow pulsation produced considerable spatial variations in the time-averaged LDL wall flux. The flow pulsation caused a continuous increase in LDL flux to the inner wall and a proximal increase in LDL flux to the outer wall followed by a constant LDL wall flux distribution in the rest of the regions. The inner wall LDL flux due to the wall motion was lower than that produced by the flow pulsatility and was actually found to decrease considerably after peaking in the medial region. Along the outer wall the LDL wall flux was lower in the proximal and medial regions and was found to steeply increase in the distal region to a value larger than that in the static model.

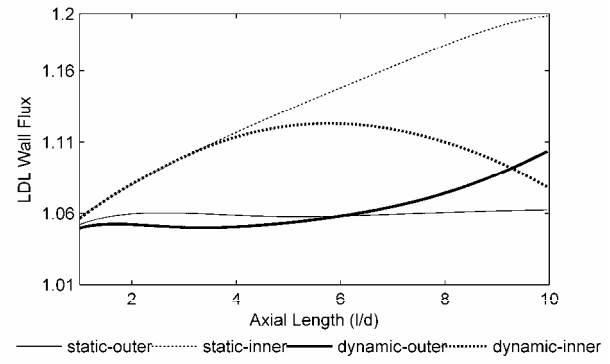

Figure 7: Time-averaged normalised LDL flux distribution along the inner and outer walls of the LAD.

Discussion

The flow patterns reported in this study qualitatively agree with the findings of past studies in that they all demonstrate velocity skewing towards the outer wall of curvature and the appearance of secondary flow [5, 18]. This basic flow feature due to the vessel curvature was further altered by the pulsatility and the wall motion. Their relative role on secondary flow can be characterised by the non-dimensional Dean number (κ).

$$\kappa = \left(\frac{d}{2R}\right)^{1/2} \mathrm{Re} \qquad (4)$$

From the definition of the Dean number, it is clear that higher the flow rate or smaller the radius of curvature the higher the Dean vortices will be. Consequently, the magnitude of skewing and the strength of Dean vortices were found to increase with increasing curvature and flow rate. Because of the time dependency of wall motion and flow rate these patterns were found to change with respect to time. The flow patterns seen in this study are qualitatively comparable to that of Santamarina et al's work which considered the effects of dynamic curvature on flow patterns [8].

Since the WSS is directly proportional to the gradient of velocity the WSS patterns predicted in the static model appeared to follow the trends of velocity distribution and are similar to those reported in other studies on pulsatile coronary artery flow [5, 18]. Consequently, the temporal WSS patterns demonstrated a clear dependence upon the flow rate curve and exhibited significant variations over the cardiac cycle. This trend was also noticed when the wall motion was introduced except in the central section where the vessel curvature was high suggesting that the effects of wall motion on temporal WSS patterns are only secondary to the pulsatile flow effects. These results also qualitatively agree with the findings of other dynamic model studies [19, 20].

The time dependent velocity skewing towards the outer wall of vessel curvature had caused steeper gradients along the outer wall when compared to the inner wall. Hence the outer and inner walls were subjected to high and low wall shear stresses respectively. Consequently, the time averaged outer WSS was larger than the inner WSS. The cumulative temporal variations in the WSS between the static and dynamic models were responsible for a higher peak and a subsequent steeper drop in the time-averaged outer WSS and a higher time-averaged inner WSS in the dynamic model when compared to the static model.

The establishment of low flow, low WSS regions along the inner wall led to an overall elevation of LDL flux and a reduction in oxygen flux to the inner wall. In contrast, high axial flow and high WSS along the outer wall caused a reduction in LDL flux and an increase in oxygen flux to the outer wall. The higher the WSS the higher the convective transport of oxygen. Hence the oxygen flux to the outer wall was more than that to the inner wall. The opposite effects were noted for LDL transport because the degree of concentration polarisation is reduced where high flow and high WSS prevail [11]. As a result, the LDL accumulation was

ISSN: 1727-1983

generally lower along the outer wall and higher along the inner wall. The diffusive transport of LDL and oxygen however, had little influence on mass transport because of their low diffusion coefficient. These results qualitatively agree with mass transport studies in curved arterial transport models [11, 18, 21].

It appears that both the flow pulsatility and the wall motion had only little effect on time dependent mass transport of LDL and oxygen. That is why neither the pulsatility nor the wall motion produced notable variations in oxygen and LDL fluxes over time. As a result, the time-averaged oxygen and LDL fluxes were only slightly different from their corresponding time dependent flux values. This less significant pulsatile effects on time-averaged mass transport patterns have also been reported by other studies [22-24]. Although the temporal mass transfer patterns in the dynamic models were not significantly affected by the wall motion, an overall change in the mass transfer patterns was evident. This change was also reflected in the time-averaged mass transfer patterns.

The mass transport patterns seemed to have been influenced by the time-averaged WSS distribution. In the proximal region, oxygen flux to the outer wall increased while that to the inner wall decreased in response to the increasing and decreasing WSS along the outer and inner walls respectively. Subsequent drop and increase in the outer and inner WSS prompted a reduction and enhancement of the time-averaged oxygen flux to the outer and inner walls in the medial to distal regions.

The LDL flux to the outer wall first increased and then decreased in response to the increasing and decreasing time-averaged WSS. In contrast, along the inner wall the LDL flux increased and then decreased in line with the inner WSS changes. In fact, the outer wall flux of LDL was higher than that to the inner wall after about 9D from the inlet. These results clearly suggest a strong dependence of LDL and oxygen transport on the time-averaged WSS distribution.

The fact that the pulsatility did not alter mass transfer patterns and the wall motion caused notable changes in species flux suggests that the wall motion may indeed be important in determining the time-averaged mass transport patterns. Such variations in species flux were only prominent in the medial and in the distal regions. This regional difference could have occured due to the specification of fixed inlet boundary condition. Nevertheless, our results indicate that the motion of coronary arteries alter the luminal mass transport patterns.

Conclusion

This study investigated the effects of idealised coronary artery motion on LDL and oxygen transport. As the transport mechanisms are different the LDL and oxygen transport were modelled with different wall boundary conditions. Our results predicted elevation of LDL flux, impaired oxygen flux and low WSS along the inner wall of curvature, a region susceptible to the formation of atherosclerosis. The temporal variations in flow and WSS patterns had little influence on species transport in the dynamic model and were secondary to the pulsatile flow effects. Nevertheless, the dynamic curvature did alter the time-averaged mass transfer in the medial and distal regions. Taken together, these results suggest that wall motion may play an important role in the coronary arterial transport processes.

References

[1] TARBELL, J. M. (2003): 'Mass transport in arteries and the localization of atherosclerosis', *Annual Review of Biomedical Engineering*, **5**, pp. 79-118.

[2] NIELSEN, L. B. (1996): 'Transfer of low density lipoprotein into the arterial wall and risk of atherosclerosis', *Atherosclerosis*, **123**, pp. 1-15.

[3] DING, J. AND FRIEDMAN, M. H. (2000): 'Dynamics of human coronary arterial motion and its potential role in coronary atherogenesis', *ASME Journal of Biomechanical Engineering*, **122**, pp. 488-492.

[4] DODGE JR, J. T., BROWN, B. G., BOLSON, E. L. AND DODGE, H. T. (1992): 'Lumen diameter of normal human coronary arteries: Influence of age, sex, anatomic variation, and left ventricular hypertrophy or dilation', *Circulation*, **86**, pp. 232-246.

[5] HE, X. AND KU, D. N. (1996): 'Pulsatile flow in the human left coronary artery bifurcation: Average conditions', *ASME Journal of Biomechanical Engineering*, **118**, pp. 74-82.

[6] GROSS, M. F. AND FRIEDMAN, M. H. (1998): 'Dynamics of coronary artery curvature obtained from biplane cineangiograms', *Journal of Biomechanics*, **31**, pp. 479-484.

[7] MARCUS, J. T., SMEENK, H. G., KUIJER, J. P. A., VAN DER GEEST, R. J., HEETHAAR, R. M. AND VAN ROSSUM, A. C. (1999): 'Flow profiles in the left anterior descending and the right coronary artery assessed by MR velocity quantification: Effects of through-plane and in-plane motion of the heart', *Journal of Computer Assisted Tomography*, **23**, pp. 567-576.

[8] SANTAMARINA, A., WEYDAHL, E., SIEGEL, J. M. AND MOORE JR, J. E. (1998): 'Computational analysis of flow in a curved tube model of the coronary arteries: Effects of time-varying curvature', *Annals of Biomedical Engineering*, **26**, pp. 944-954.

[9] MA, P., LI, X. AND KU, D. N. (1997): 'Convective mass transfer at the carotid bifurcation', *Journal of Biomechanics*, **30**, pp. 565-571.

[10] STANGEBY, D. K. AND ETHIER, C. R. (2002): Computational analysis of coupled blood-wall arterial LDL transport, *ASME Journal of Biomechanical Engineering*, **124**, pp. 1-8.

[11] WADA, S. AND KARINO, T. (2002): 'Theoretical prediction of low-density lipoproteins

ISSN: 1727-1983

concentration at the luminal surface of an artery with a multiple bend', *Annals of Biomedical Engineering*, **30**, pp. 778-791.

[12] WILENS, S. L. AND MCCLUSKEY, R. T. (1952): 'The comparative filtration properties of excised arteries and veins', *The American Journal of the Medical Sciences*, **224**, pp. 540-547.

[13] BACK, L. H. (1975): 'Theoretical investigation of mass transport to arterial walls in various blood flow regions-I. Flow field and lipoprotein transport', *Mathematical Biosciences*, **27**, pp. 231-262.

[14] TRUSKEY, G. A., ROBERTS, W. L., HERRMANN, R. A. AND MALINAUSKS, R. A. (1992): 'Measurement of endothelial permeability to ^{125}I-low density lipoproteins in rabbit arteries by use of en face preparations', *Circulation Research*, **71**, pp. 883-897.

[15] BACK, L. H. (1975): 'Theoretical investigation of mass transport to arterial walls in various blood flow regions-II. Oxygen transport and its relationship to lipoprotein accumulation', *Mathematical Biosciences*, **27**, pp. 263-285.

[16] FRIEDMAN, M. H. AND EHRLICH, L. W. (1975): 'Effect of spatial variations in shear on diffusion at the wall of an arterial branch', *Circulation Research*, **37**, pp. 446-454.

[17] KOLANDAVEL, M. K., FRUEND, E. T., RINGGAARD, S. AND WALKER, P. G. (2005): 'The effects of time varying curvature on species transport in coronary arteries', *Annals of Biomedical Engineering*, (submitted).

[18] QIU, Y. AND TARBELL, J. M. (2000): 'Numerical simulation of pulsatile flow in a compliant curved tube model of a coronary artery', *ASME Journal of Biomechanical Engineering*, **122**, pp. 77-85.

[19] ZENG, D., DING, Z., FRIEDMAN, M. H. AND ETHIER, C. R. (2003): 'Effects of cardiac motion on right coronary hemodynamics', *Annals of Biomedical Engineering*, **31**, pp. 420-429.

[20] PROSI, M., PERKTOLD, K., DING, J. AND FRIEDMAN, M. H. (2004): 'Influence of curvature dynamics on pulsatile coronary artery flow in a realistic bifurcation model', *Journal of Biomechanics*, **37**, pp. 1767-1775.

[21] KAAZEMPUR-MOFRAD, M. R. AND ETHIER, C. R. (2001): 'Mass transport in an anatomically realistic human right coronary artery', *Annals of Biomedical Engineering*, **29**, pp. 121-127.

[22] SCHNEIDERMAN, G., MOCKROS, L. F. AND GOLDSTICK, T. K. (1982): 'Effect of pulsatility on oxygen transport to the human arterial wall', *Journal of Biomechanics*, **15**, pp. 849-858.

[23] MA, P., LI, X. AND KU, D. N. (1994): 'Heat and mass transfer in a separated flow region for high Prandtl and Schmidt numbers under pulsatile flow conditions', *International Journal of Heat and Mass Transfer*, **37**, pp. 2723-2736.

[24] FATOURAEE, A., DENG, X., DE CHAMPLAIN, A. AND GUIDOIN, R. (1998): 'Concentration polarization of low density lipoproteins (LDL) in the arterial system', *Annals of the New York Academy of Sciences*, **858**, pp. 137-146.

ISSN: 1727-1983